First-Order Phase Transition Interpretation of Pulsar Timing Array Signal Is Consistent with Solar-Mass Black Holes

Yann Gouttenoire*
School of Physics and Astronomy, Tel-Aviv University, Tel-Aviv 69978, Israel

(Received 12 July 2023; accepted 8 September 2023; published 26 October 2023)

We perform a Bayesian analysis of NANOGrav 15-yr and IPTA DR2 pulsar timing residuals and show that the recently detected stochastic gravitational-wave background is compatible with a stochastic gravitational-wave background produced by bubble dynamics during a cosmological first-order phase transition. The timing data suggest that the phase transition would occur around QCD confinement temperature and would have a slow rate of completion. This scenario can naturally lead to the abundant production of primordial black holes with solar masses. These primordial black holes can potentially be detected by current and advanced gravitational-wave detectors LIGO-Virgo-Kagra, Einstein Telescope, Cosmic Explorer, by astrometry with GAIA, and by 21-cm survey.

DOI: 10.1103/PhysRevLett.131.171404

Introduction.—By measuring cross-correlations in the arrival times of pulses emitted by rotating neutron stars, pulsar timing arrays (PTAs) have been established as a mean to detect nanohertz frequency gravitational waves (GW). In 2020, a common low-frequency noise has been identified in the datasets of NANOGrav 12.5-yr [1], EPTA DR1 [2], and PPTA DR2 [3], and confirmed in 2022 by IPTA DR2 [4], which combines data from the former. To distinguish a GW origin from systematic effects requires timing delay correlations to have a quadrupolar dependence on the angular separation between pulsars [5]. In June 2023, following the analysis of their most recent data, the collaborative efforts of NANOGrav 15-yr (NG15), EPTA DR2, and PPTA DR3 have identified compelling statistical evidence for such interpulsar correlations [6–8], with Bayes factors of 600, 60, and 11, respectively. The primary expected source of GWs at low frequencies is believed to be from supermassive black hole (SMBH) binaries [9–11]. The stochastic GW background (SGWB) inferred from PTA data corresponds to the upper limit of the astrophysical predicted interval; see Fig. 1. Recent studies suggest the possibility of SMBH binaries being slightly more massive and more numerous than initially anticipated [12–15]. Alternatively, the PTA SGWB might originate from new physics taking place in the early Universe [15–18]. The last hypothesis, however, comes with its own set of challenges. For instance, ascribing the SGWB to inflation necessitates unnaturally large values for the spectral tilt $n_t \simeq 1.8$ and a low reheating temperature $T_{\rm reh} \lesssim 10$ GeV [19]. GWs induced by a Gaussian spectrum of curvature perturbation would result in excessive primordial black hole (PBH) production [20,21], same for a SGWB produced from domain wall annihilation [22]. A SGWB resulting from PBH mergers would not align with structure formation [23,24]. A cosmic strings network, when arising from a global symmetry is excluded by big-bang nucleosynthesis (BBN) [25–28], while when arising from a local symmetry is not favored by the Bayesian analysis [16,29]. To evade BBN bound, a first-order phase transition (1stOPT) sourcing PTA signal would necessitate the latent heat to be released dominantly to the standard model, e.g., [15–18,30–33]. Interestingly, however, the 1stOPT interpretation of PTA SGWB requires a reheating temperature around the scale of QCD confinement 100 MeV, with a rather low completion rate $\beta/H \lesssim 12$ and a large latent heat fraction $\alpha \gtrsim 0.5$ [16]. This overlaps with the region where 1stOPTs have been recently found to produce PBHs in observable amount [34]. The PBH prior has been omitted in all previous analysis of the 1stOPT interpretation of PTA data [15–18,30–33,35–46].

In this Letter, we perform a Bayesian search for SGWB from 1stOPT in NANOGrav 15-year (NG15) and IPTA DR2 (IPTA2) timing residuals, including both BBN-$N_{\rm eff}$-bound and PBH-overproduction constraints as priors in the analysis. To simplify the numerical strategy, we focus on the region $\alpha \gg 1$ of strong supercooling where PBH production is the most efficient. (The Bayesian analysis of 1stOPT with finite α will be presented elsewhere.) We argue that the SGWB from 1stOPT is given by the bulk flow model independently of whether the latent heat is still stored in bubble walls at percolation or has been released to the plasma before. We find that PBH formation does not exclude the 1stOPT interpretation of PTA signal. Instead, a SGWB from supercooled phase transition (PT) is favored

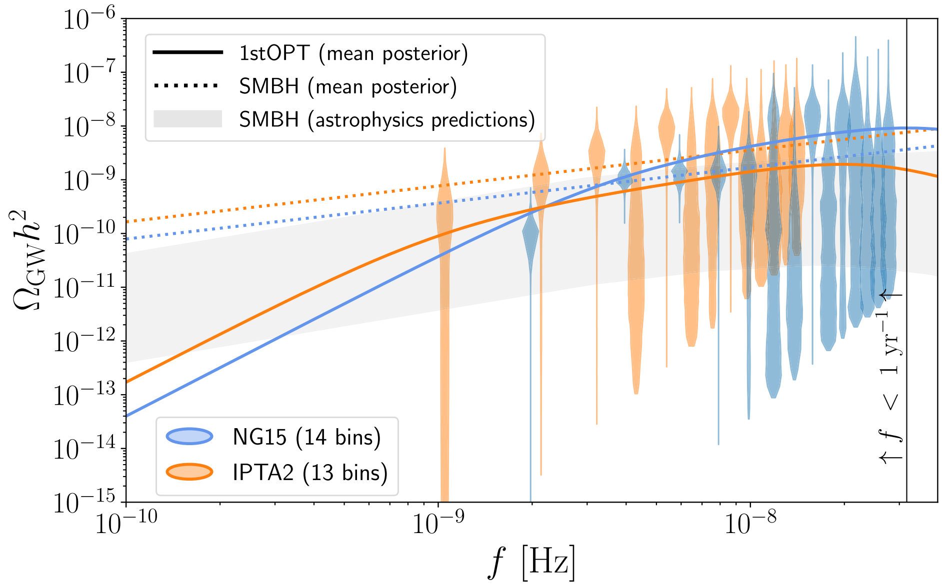

FIG. 1. The "violin" diagrams depict the posterior probability distribution of the SGWB energy density in each frequency bins of NG15 and IPTA2 datasets. We overlay with solid lines the SWGB from 1stOPT using mean posterior value for the PT parameters, cf. Supplemental Material [47]. The dotted lines illustrate the SGWB originating from SMBH binaries, employing the mean posterior value for the amplitude and fixing the power-law index to $\beta = 2/3$. The gray band represents the 90% confidence interval for the projected SGWB based on a Monte Carlo simulation of a binary population of SMBHs [72].

with respect to the SMBH binary hypothesis by a Bayes factor of 15 in NG15 dataset. We show, for the first time, the existence of a multimessenger window: the NG15 posterior contains a region producing (0.1–10) solar-mass PBHs; see Fig. 3. The merging of such PBHs would source GWs with kHz frequencies in the range of LIGO-Virgo [73–77] and ET/CE [78,79]. Additionally, their presence could be detected from lensing in GAIA [80–82] or from heating in 21-cm survey [83–85].

We also consider the negative hypothesis in which the SGWB observed in PTA would not result from a supercooled PT and derive lower limits on the rate of completion $\beta/H \gtrsim [10\text{–}20]$, implying that the Universe could not have boiled longer than (5%–10%) of a Hubble time during the QCD phase transition.

Gravitational waves from first-order PT.—PT parameters: The strength of a 1stOPT is characterized by the ratio of its latent heat ΔV, defined as the vacuum energy difference between the two minima of the potential driving the transition, to the radiation energy density $\rho_{\rm rad}(T_n)$ at the nucleation temperature T_n

$$\alpha \equiv \frac{\Delta V}{\rho_{\rm rad}(T_n)} \equiv \left(\frac{T_{\rm eq}}{T_{\rm n}}\right)^4, \tag{1}$$

where we have neglected a ratio of number of relativistic degrees of freedom. A 1stOPT is said supercooled when $\alpha \gtrsim 1$, in which case the Universe enters a stage of vacuum domination at temperature $T_{\rm eq}$ that ends at T_n when bubble growth converts the latent heat into radiation energy density. The rate at which nucleation takes place is controlled by the time derivative of the tunneling rate per unit of volume Γ_V

$$\beta \equiv \frac{1}{\Gamma_V}\frac{d\Gamma_V}{dt}. \tag{2}$$

After the phase transition completes, the Universe is reheated back to the temperature $T_{\rm eq}$ up to changes in number of degrees of freedom that we neglect.

GW signal: The dynamics of weak 1stOPT $\alpha < 1$ is rather well-understood: the latent heat is transferred to sound waves [86–93] and turbulence [94–98], which are both known for sourcing GWs [99,100]. The dynamics of strong 1stOPT $\alpha > 1$ is more complex due to the large Lorentz factor $\gamma_w \gg 1$ of bubble walls [101,102]. In the scenario where the friction pressure is small, the latent heat is dominantly transferred to kinetic energy of bubble walls. The SGWB from bubble collision is known to be given by the bulk flow model [103–107], which succeeds the envelope approximation [108–112]. In the scenario where the bubble reaches a terminal velocity due to the friction pressure, the latent heat is transferred to the plasma in terms of relativistic shock waves [113] and relativistic free-streaming particles [102,114–117]. Because of Lorentz contraction, their momentum distribution is highly peaked and from a gravitational point of view, they should be indistinguishable from infinitely thin bubble walls. For this reason, the SGWB from strong 1stOPT $\alpha > 1$ should be well approximated by the bulk flow model. We consider the supercooled limit $\alpha \gg 1$ in which the dependency of the GW signal on both the wall velocity ($v_w = 1$) and the latent

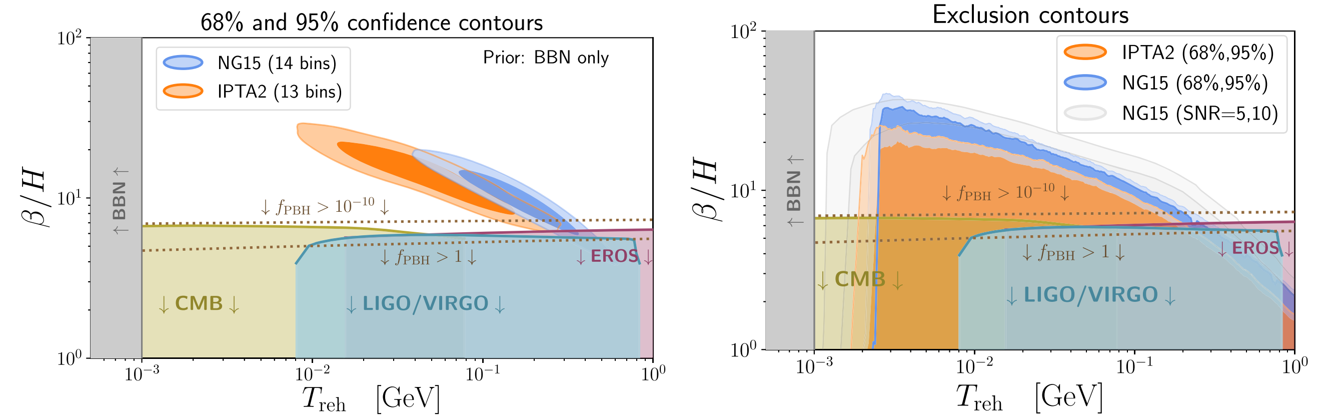

FIG. 2. Left: colored regions are posterior distributions in term of the reheating temperature $T_{\rm reh}$ and rate of completion β/H of a strong 1stOPT ($\alpha \gg 1$). They are obtained after performing a Bayesian analysis of PTA dataset. We overlay the CMB, LIGO-Virgo. and microlensing (EROS) constraints on PBHs produced during such 1stOPT. Right: lower limit on the rate of completion β/H in the negative hypothesis in which the PTA SGWB would not arise from a strong PT ($\alpha \gg 1$). We cast 68% and 95% lower limit using Bayesian inference as explained in the Supplemental Material [47] (orange and blue), or using the power-law integrated curve in [128] (gray) assuming a signal-to-noise ratio (SNR) threshold of 5 and 10.

heat fraction α disappears. The SGWB spectrum, including additional details, can be found in the Supplemental Material [47].

PTA data analysis.—Numerical strategy: We searched for GW from 1stOPT in two open-access datasets, NG15 [6] and IPTA2 [4]. The released data are presented in terms of the timing-residual cross-power spectral density $S_{ab}(f) \equiv \Gamma_{ab} h_c^2(f)/(12\pi^2) f^{-3}$, where $h_c(f) \simeq 1.26 \times 10^{-18}\ (\mathrm{Hz}/f)\sqrt{h^2\Omega_{\rm GW}(f)}$ signifies the characteristic strain spectrum [118] and Γ_{ab} denotes the overlap reduction function between pulsars "a" and "b" within a given PTA [119]. We used the software packages ENTERPRISE [120] and ENTERPRISE_EXTENSIONS [121] to compute the likelihood of observing given timing residuals assuming the presence of the SGWB from 1stOPT given in the Supplemental Material [47]. We used PTMCMC [122] to generate the posterior distribution. For IPTA2, we marginalized over white, red, and dispersion measure noises as prescribed in [4,20,123]. For NG15, we instead used the handy wrapper PTArcade [124] with "enterprise" mode in which marginalization over noise parameters is automatized. We used GetDist [125] tool to plot the results. To circumvent pulsar-intrinsic excess noise at high frequencies, the SGWB search was confined to the lowest 14 and 13 frequency bins of the NG15 and IPTA2 datasets, respectively. We included the BBN constraints assuming that the 1stOPT sector reheats dominantly into standard model degrees of freedom and, when specified, the one from PBH overproduction, discussed in the "Primordial Black Holes" section, to infer the prior distribution of 1stOPT parameters. Detailed information regarding data analysis and prior choices can be found in the Supplemental Material [47].

Supercooled PT: We conducted searches for GW from strong 1stOPT ($\alpha \gg 1$) in isolation, GW from SMBH binaries individually, as well as a combined analysis of 1stOPT and SMBH binaries. In Fig. 1, we show the GW spectra with parameters set to their mean posterior values given in the table of the Supplemental Material [47]. The 68% and 95% confidence contours are depicted in Fig. 2 (left). The posterior for the combined analysis of 1stOPT and SMBH is reported to the Supplemental Material [47]. We assumed a flat prior on the strain amplitude of the SGWB from SMBH binaries, as well as the spectral slope of 13/3 associated with GW-driven inspirals. To quantify the evidence provided by the observed PTA data, denoted as $\mathcal{D}$, in favor of one model, say X, versus another, say Y, we employ the Bayesian factor

$$\mathrm{BF}_{Y,X} \equiv \mathcal{P}(\mathcal{D}|Y)/\mathcal{P}(\mathcal{D}/X), \tag{3}$$

which we compute using the product-space sampling method [119] implemented in ENTERPRISE_EXTENSIONS [121]. Here, $\mathcal{P}(\mathcal{D}/X)$ is the likelihood probability of observing data $\mathcal{D}$ given the model X. The outcomes of the Bayesian model comparison presented in Table I,

TABLE I. Bayesian factors $\mathrm{BF}_{Y,X}$ with values significantly exceeding 1 indicate support for interpretation Y with respect to X. Conversely, values approaching 1 suggest no discernible preference between X and Y. We can see that the 1stOPT interpretation is favored with respect to SMBH binaries in NG15 data and that the PBH prior only slightly worsens the fit.

			$\mathrm{BF}_{Y,X}$	
Model X	Model Y	Prior	NG15	IPTA2
SMBH	1stOPT	BBN	24	0.50
		BBN + PBH	15	0.49
SMBH	SMBH + 1stOPT	BBN + PBH	9.3	1.2

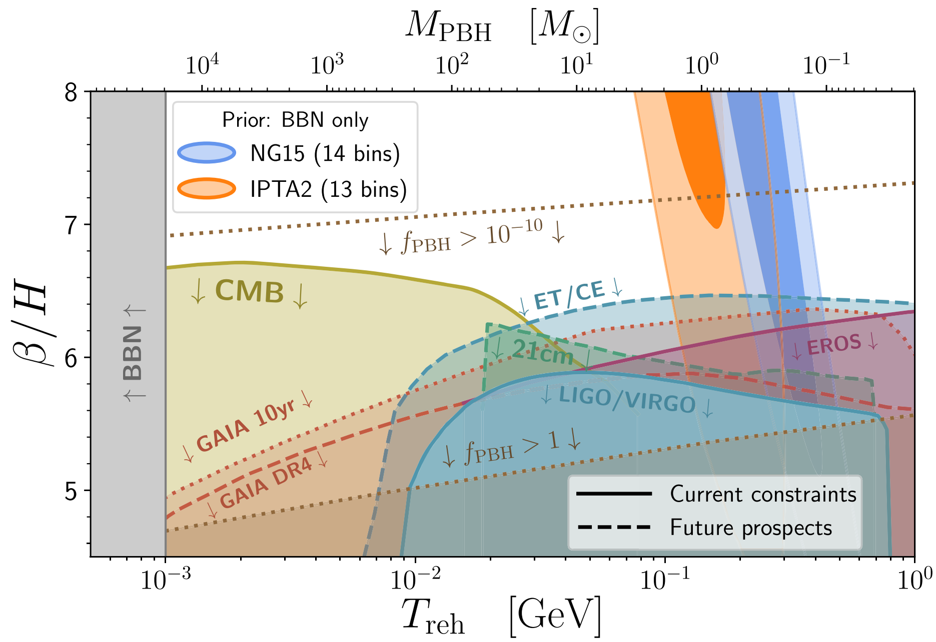

FIG. 3. The ellipses are the posterior distributions obtained after a Bayesian search of SGWB sourced by a supercooled 1stOPT in NG15 and IPTA2 datasets. We overlay the region producing PBHs detectable by different observatories; see the "Primordial Black Holes" section for details.

according to Jeffrey's scale [126,127], suggest that NG15 data "substantially" favors the presence of a GW signal from 1stOPT aside to the one from SMBH. Instead, IPTA2 data remains inconclusive.

Exclusion bounds: Under the assumption that the PTA signal does not arise from 1stOPT, we have derived upper limits on the GW signal emanating from 1stOPT. As depicted in Fig. 2 (right), these limits correspond to lower bounds on the rate of completion, going up to $\beta/H \lesssim 20$. As discussed in the Supplemental Material [47], these lower limits are conservative as the GW spectrum from SMBH was not included in the analysis.

Primordial black holes.—Supercooled late-blooming mechanism: In [34], it was demonstrated that PBHs could be produced in observable amount during supercooled PT through a process termed "late-blooming." During 1stOPT, the nucleation sites of bubbles are randomly dispersed across the entire volume of the false vacuum. As the Universe gets close to the point of percolation, there remains a nonzero probability of identifying Hubble-sized regions where nucleation has not yet initiated. Throughout the supercooled PT, these delayed regions maintain a constant vacuum energy, while the energy density in their vicinity redshifts like radiation. Upon completion of percolation, these "late-bloomers" evolve into overdense regions. If these regions are Hubble-sized and exceed a certain density threshold $\delta\rho/\rho \gtrsim 0.45$, they collapse into PBHs. We direct the reader to [34] for the precise analytical formula to estimate the abundance and mass of those PBHs. (Some other works [129–132] find a different PBH abundance. References [129,130,132] find a lower PBH abundance because the formalism is restricting collapsing patch to remain 100% vacuum dominated until collapse. Reference [131] finds a larger abundance because nucleation is not accounted in the entire past light cone of a collapsing patch. Instead, Ref. [34] accounts for nucleation to take place not only in the whole past light cone but also in the collapsing patch itself as long as the critical overdensity is reached.) The mass distribution of those PBHs, left for future studies in [34], is assumed to resemble a delta function in the present work. We included the PBH overproduction constraints as a prior in the Bayesian analysis. The Bayes factors shown in Table I are unaffected for IPTA2 and only decrease from 24 to 15 for NG15. We have plotted the contour lines representing the PBH fraction of dark matter $f_{\rm PBH}$ in Fig. 2 and the PBH mass in Fig. 3. In addition, we overlay cosmological and astrophysical constraints on this population of PBHs.

Excluded regions and detection prospects: With solid lines, we show current constraints. In yellow, we have the exclusion regions arising from distortion of the cosmic microwave background (CMB) caused by x rays from accretion that modify the ionization history between recombination and reionization [133–135]. In purple, we show the constraints using the search for photometric magnification (strong lensing) of stars in the Magellanic clouds conducted on Eros data [136]. The solid cyan-colored region represents constraints derived from the data collected by LIGO-Virgo interferometers [73–77]. With dashed lines, we show future prospects. In green, we have the reach of 21-cm surveys due to heating and ionization of the intergalactic medium via x rays produced during accretion [83–85]. In red, we have the forecast from the search for transient astrometric deviation (weak lensing) of single or multiple stars in GAIA time-series data [80–82]. Finally, in dashed cyan we show the prospect for detecting GW from PBH binaries with Einstein telescope and Cosmic Explorer [78,79].

Conclusion.—We conducted a Bayesian analysis of the NANOGrav 15-yr (NG15) and IPTA DR2 (IPTA2) timing residuals. Our findings indicate that NG15 indicate a substantial preference for the presence of a strong first-order phase transitions (1stOPT) in isolation or combined with SGWB from SMBH binaries, while IPTA2 remains inconclusive on which scenario is preferred. The phase transition is characterized by a remarkably low completion rate, e.g., $\beta/H \simeq 12.6$ and 10.7 for NG15 with and without astrophysical signal from SMBH binaries. From a theoretical perspective, such a value is typical of supercooled phase transitions, characterized by a strong first-order phase transition with a parameter α significantly larger than 1, e.g., [99,100,137], which motivates the choice of prior $\alpha \gg 1$ done in this Letter. These cosmological scenarios have been demonstrated to produce primordial black holes (PBHs) in considerable quantities when $\beta/H \lesssim 7$ [34]. We checked that in contrast to the scalar-induced [20,21] and domain-wall [22] interpretations of PTA signal, the 1stOPT interpretation does not fall into the PBH graveyard of PTA's interpretations. The Bayes factor of the strong 1stOPT interpretation with respect to SMBH binary one is only reduced from 24 to 15 in NG15 after including the PBH prior, while it is not affected in IPTA2. However, we showed that the 1stOPT interpretation of the PTA signal might be associated with the presence of solar-mass PBHs in our Universe today. We further assessed the potential for detecting these PBHs using different observational techniques, including 21-cm cosmological hydrogen line observations, astrometry with the GAIA mission, and next-generation kilohertz frequency GW interferometers such as the Einstein Telescope and Cosmic Explorer. In the event that an astrophysical explanation becomes definitive, we established 68% and 95% exclusion constraints on the parameter space of 1stOPT, up until $\beta/H \gtrsim 20$. Under these conditions, it would effectively preclude any possibility of detecting PBHs from supercooled PTs within the mass range $(1M_\odot, 10^3 M_\odot]$; see Supplemental Material [47].

The author is grateful to Iason Baldes, Ryusuke Jinno, Marius Kongsore, Fabrizio Rompineve, Miguel Vanvlasselaer, and Tomer Volansky for fruitful discussions and to the Azrieli Foundation for the award of an Azrieli Fellowship.

[*]Corresponding author: yann.gouttenoire@gmail.com

[1] N. S. Pol *et al.* (NANOGrav Collaboration), Astrophysics milestones for pulsar timing array gravitational-wave detection, Astrophys. J. Lett. **911**, L34 (2021).

[2] S. Chen *et al.*, Common-red-signal analysis with 24-yr high-precision timing of the European pulsar timing array: Inferences in the stochastic gravitational-wave background search, Mon. Not. R. Astron. Soc. **508**, 4970 (2021).

[3] B. Goncharov *et al.*, On the evidence for a common-spectrum process in the search for the nanohertz gravitational-wave background with the Parkes pulsar timing array, Astrophys. J. Lett. **917**, L19 (2021).

[4] J. Antoniadis *et al.*, The International pulsar timing array second data release: Search for an isotropic gravitational wave background, Mon. Not. R. Astron. Soc. **510**, 4873 (2022).

[5] R. w. Hellings and G. s. Downs, Upper limits on the isotropic gravitational radiation background from pulsar timing analysis, Astrophys. J. Lett. **265**, L39 (1983).

[6] G. Agazie *et al.* (NANOGrav Collaboration), The NANOGrav 15 yr data set: Evidence for a gravitational-wave background, Astrophys. J. Lett. **951**, L8 (2023).

[7] J. Antoniadis *et al.*, The second data release from the European pulsar timing array III. Search for gravitational wave signals, arXiv:2306.16214.

[8] D. J. Reardon *et al.*, Search for an isotropic gravitational-wave background with the Parkes pulsar timing array, Astrophys. J. Lett. **951**, L6 (2023).

[9] A. Sesana, Insights into the astrophysics of supermassive black hole binaries from pulsar timing observations, Classical Quantum Gravity **30**, 224014 (2013).

[10] L. Z. Kelley, L. Blecha, L. Hernquist, A. Sesana, and S. R. Taylor, The gravitational wave background from massive black hole binaries in illustris: Spectral features and time to detection with pulsar timing arrays, Mon. Not. R. Astron. Soc. **471**, 4508 (2017).

[11] S. Chen, A. Sesana, and C. J. Conselice, Constraining astrophysical observables of galaxy and supermassive black hole binary mergers using pulsar timing arrays, Mon. Not. R. Astron. Soc. **488**, 401 (2019).

[12] H. Middleton, A. Sesana, S. Chen, A. Vecchio, W. Del Pozzo, and P. A. Rosado, Massive black hole binary systems and the NANOGrav 12.5 yr results, Mon. Not. R. Astron. Soc. **502**, L99 (2021).

[13] J. A. Casey-Clyde, C. M. F. Mingarelli, J. E. Greene, K. Pardo, M. Nañez, and A. D. Goulding, A quasar-based supermassive black hole binary population model: Implications for the gravitational wave background, Astrophys. J. **924**, 93 (2022).

[14] G. Agazie *et al.* (NANOGrav Collaboration), The NANOGrav 15-year data set: Constraints on supermassive black hole binaries from the gravitational wave background, Astrophys. J. Lett. **952**, L37 (2023).

[15] J. Antoniadis *et al.*, The second data release from the European pulsar timing array: V. Implications for massive black holes, dark matter and the early Universe, arXiv:2306.16227.

[16] A. Afzal *et al.* (NANOGrav Collaboration), The NANOGrav 15 yr data set: Search for signals from new physics, Astrophys. J. Lett. **951**, L11 (2023).

[17] E. Madge, E. Morgante, C. P. Ibáñez, N. Ramberg, and S. Schenk, Primordial gravitational waves in the nano-Hertz regime and PTA data—towards solving the GW inverse problem, arXiv:2306.14856.

[18] D. G. Figueroa, M. Pieroni, A. Ricciardone, and P. Simakachorn, Cosmological background interpretation of pulsar timing array data, arXiv:2307.02399.

[19] S. Vagnozzi, Inflationary interpretation of the stochastic gravitational wave background signal detected by pulsar timing array experiments, J. High Energy Astrophys. **39**, 81 (2023).

[20] V. Dandoy, V. Domcke, and F. Rompineve, Search for scalar induced gravitational waves in the international pulsar timing array data release 2 and NANOgrav 12.5 years dataset, arXiv:2302.07901.

[21] G. Franciolini, A. Iovino, Junior., V. Vaskonen, and H. Veermae, The recent gravitational wave observation by pulsar timing arrays and primordial black holes: The importance of non-gaussianities, arXiv:2306.17149.

[22] Y. Gouttenoire and E. Vitagliano, Domain wall interpretation of the PTA signal confronting black hole overproduction, arXiv:2306.17841.

[23] Y. Gouttenoire, S. Trifinopoulos, G. Valogiannis, and M. Vanvlasselaer, Scrutinizing the primordial black holes interpretation of PTA gravitational waves and JWST early galaxies, arXiv:2307.01457.

[24] P. F. Depta, K. Schmidt-Hoberg, and C. Tasillo, Do pulsar timing arrays observe merging primordial black holes?, arXiv:2306.17836.

[25] M. Gorghetto, E. Hardy, and H. Nicolaescu, Observing invisible axions with gravitational waves, J. Cosmol. Astropart. Phys. 06 (2021) 034.

[26] C.-F. Chang and Y. Cui, Gravitational waves from global cosmic strings and cosmic archaeology, J. High Energy Phys. 03 (2022) 114.

[27] J. A. Dror, H. Murayama, and N. L. Rodd, Cosmic axion background, Phys. Rev. D **103**, 115004 (2021); **106**, 119902(E) (2022).

[28] G. Servant and P. Simakachorn, Constraining Post-inflationary axions with pulsar timing arrays, arXiv:2307.03121.

[29] J. Ellis, M. Lewicki, C. Lin, and V. Vaskonen, Cosmic superstrings revisited in light of NANOGrav 15-year data, arXiv:2306.17147.

[30] W. Ratzinger and P. Schwaller, Whispers from the dark side: Confronting light new physics with NANOGrav data, SciPost Phys. **10**, 047 (2021).

[31] Z. Arzoumanian *et al.* (NANOGrav Collaboration), Searching for gravitational waves from cosmological phase transitions with the NANOGrav 12.5-year dataset, Phys. Rev. Lett. **127**, 251302 (2021).

[32] Y. Bai and M. Korwar, Cosmological constraints on first-order phase transitions, Phys. Rev. D **105**, 095015 (2022).

[33] T. Bringmann, P. F. Depta, T. Konstandin, K. Schmidt-Hoberg, and C. Tasillo, Does NANOGrav observe a dark sector phase transition?, arXiv:2306.09411.

[34] Y. Gouttenoire and T. Volansky, Primordial black holes from supercooled phase transitions, arXiv:2305.04942.

[35] Y. Nakai, M. Suzuki, F. Takahashi, and M. Yamada, Gravitational waves and dark radiation from dark phase transition: Connecting NANOGrav pulsar timing data and hubble tension, Phys. Lett. B **816**, 136238 (2021).

[36] A. Addazi, Y.-F. Cai, Q. Gan, A. Marciano, and K. Zeng, NANOGrav results and dark first order phase transitions, Sci. China Phys. Mech. Astron. **64**, 290411 (2021).

[37] C. J. Moore and A. Vecchio, Ultra-low-frequency gravitational waves from cosmological and astrophysical processes, Nat. Astron. **5**, 1268 (2021).

[38] S.-L. Li, L. Shao, P. Wu, and H. Yu, NANOGrav signal from first-order confinement-deconfinement phase transition in different QCD-matter scenarios, Phys. Rev. D **104**, 043510 (2021).

[39] A. Brandenburg, E. Clarke, Y. He, and T. Kahniashvili, Can we observe the QCD phase transition-generated gravitational waves through pulsar timing arrays?, Phys. Rev. D **104**, 043513 (2021).

[40] A. Roper Pol, C. Caprini, A. Neronov, and D. Semikoz, Gravitational wave signal from primordial magnetic fields in the pulsar timing array frequency band, Phys. Rev. D **105**, 123502 (2022).

[41] K. Fujikura, S. Girmohanta, Y. Nakai, and M. Suzuki, NANOGrav signal from a dark conformal phase transition, arXiv:2306.17086.

[42] A. Addazi, Y.-F. Cai, A. Marciano, and L. Visinelli, Have pulsar timing array methods detected a cosmological phase transition?, arXiv:2306.17205.

[43] Y. Xiao, J. M. Yang, and Y. Zhang, Implications of Nano-hertz gravitational waves on electroweak phase transition in the singlet dark matter model, arXiv:2307.01072.

[44] T. Ghosh, A. Ghoshal, H.-K. Guo, F. Hajkarim, S. F. King, K. Sinha, X. Wang, and G. White, Did we hear the sound of the Universe boiling? Analysis using the full fluid velocity profiles and NANOGrav 15-year data, arXiv:2307.02259.

[45] A. Yang, J. Ma, S. Jiang, and F. P. Huang, Implication of nano-Hertz stochastic gravitational wave on dynamical dark matter through a first-order phase transition, arXiv:2306.17827.

[46] P. Athron, A. Fowlie, C.-T. Lu, L. Morris, L. Wu, Y. Wu, and Z. Xu, Can supercooled phase transitions explain the gravitational wave background observed by pulsar timing arrays?, arXiv:2306.17239.

[47] See Supplemental Material at http://link.aps.org/supplemental/10.1103/PhysRevLett.131.171404 for more details on the GW spectrum from supercooled 1stOPT and on the analysis of PTA datasets, which includes Refs. [48–71].

[48] R. Durrer and C. Caprini, Primordial magnetic fields and causality, J. Cosmol. Astropart. Phys. 11 (2003) 010.

[49] C. Caprini, R. Durrer, T. Konstandin, and G. Servant, General properties of the gravitational wave spectrum from phase transitions, Phys. Rev. D **79**, 083519 (2009).

[50] R.-G. Cai, S. Pi, and M. Sasaki, Universal infrared scaling of gravitational wave background spectra, Phys. Rev. D **102**, 083528 (2020).

[51] A. Hook, G. Marques-Tavares, and D. Racco, Causal gravitational waves as a probe of free streaming particles and the expansion of the universe, J. High Energy Phys. 02 (2021) 117.

[52] T. N. Collaboration, The nanograv 15-year data set, 10.5281/zenodo.8104459 (2023); for a full author list, see: Gabriella Agazie *et al.* Astrophys. J. Lett. **951**, L9 (2023).

[53] S. Ransom and the IPTADR2 team, https://gitlab.com/IPTA/DR2/-/tree/master/release/VersionB.

[54] Z. Arzoumanian *et al.* (NANOGrav Collaboration), The NANOGrav nine-year data set: Observations, arrival time measurements, and analysis of 37 millisecond pulsars, Astrophys. J. **813**, 65 (2015).
[55] M. L. Jones *et al.*, The NANOGrav nine-year data set: Measurement and analysis of variations in dispersion measures, Astrophys. J. **841**, 125 (2017).
[56] G. Agazie *et al.* (NANOGrav Collaboration), The NANOGrav 15-year data set: Observations and timing of 68 millisecond pulsars, Astrophys. J. Lett. **951**, L9 (2023).
[57] Z. Arzoumanian *et al.* (NANOGrav Collaboration), The NANOGrav 12.5 yr data set: Search for an isotropic stochastic gravitational-wave background, Astrophys. J. Lett. **905**, L34 (2020).
[58] A. Chalumeau *et al.*, Noise analysis in the European pulsar timing array data release 2 and its implications on the gravitational-wave background search, Mon. Not. R. Astron. Soc. **509**, 5538 (2021).
[59] R. L. Workman *et al.* (Particle Data Group), Review of particle physics, Prog. Theor. Exp. Phys. **2022**, 083C01 (2022).
[60] G. Mangano and P. D. Serpico, A robust upper limit on N_{eff} from BBN, circa 2011, Phys. Lett. B **701**, 296 (2011).
[61] A. Peimbert, M. Peimbert, and V. Luridiana, The primordial helium abundance and the number of neutrino families, Rev. Mex. Astron. Astrofis. **52**, 419 (2016).
[62] G. Mangano, G. Miele, S. Pastor, T. Pinto, O. Pisanti, and P. D. Serpico, Relic neutrino decoupling including flavor oscillations, Nucl. Phys. **B729**, 221 (2005).
[63] P. F. de Salas and S. Pastor, Relic neutrino decoupling with flavour oscillations revisited, J. Cosmol. Astropart. Phys. 07 (2016) 051.
[64] C. Pitrou, A. Coc, J.-P. Uzan, and E. Vangioni, Precision big bang nucleosynthesis with improved Helium-4 predictions, Phys. Rep. **754**, 1 (2018).
[65] C. Dvorkin *et al.*, The physics of light relics, in *2022 Snowmass Summer Study* (2022), arXiv:2203.07943.
[66] M. Kawasaki, K. Kohri, and N. Sugiyama, MeV scale reheating temperature and thermalization of neutrino background, Phys. Rev. D **62**, 023506 (2000).
[67] T. Hasegawa, N. Hiroshima, K. Kohri, R. S. L. Hansen, T. Tram, and S. Hannestad, MeV-scale reheating temperature and thermalization of oscillating neutrinos by radiative and hadronic decays of massive particles, J. Cosmol. Astropart. Phys. 12 (2019) 012.
[68] E. S. Phinney, A practical theorem on gravitational wave backgrounds, arXiv:astro-ph/0108028.
[69] J. D. Romano and N. J. Cornish, Detection methods for stochastic gravitational-wave backgrounds: A unified treatment, Living Rev. Relativity **20**, 2 (2017).
[70] W. G. Lamb, S. R. Taylor, and R. van Haasteren, The need for speed: Rapid refitting techniques for bayesian spectral characterization of the gravitational wave background using PTAs, arXiv:2303.15442.
[71] J. Ellis, M. Lewicki, J. M. No, and V. Vaskonen, Gravitational wave energy budget in strongly supercooled phase transitions, J. Cosmol. Astropart. Phys. 06 (2019) 024.
[72] P. A. Rosado, A. Sesana, and J. Gair, Expected properties of the first gravitational wave signal detected with pulsar timing arrays, Mon. Not. R. Astron. Soc. **451**, 2417 (2015).
[73] T. Nakamura, M. Sasaki, T. Tanaka, and K. S. Thorne, Gravitational waves from coalescing black hole MACHO binaries, Astrophys. J. Lett. **487**, L139 (1997).
[74] M. Raidal, C. Spethmann, V. Vaskonen, and H. Veermäe, Formation and evolution of primordial black hole binaries in the early universe, J. Cosmol. Astropart. Phys. 02 (2019) 018.
[75] B. J. Kavanagh, D. Gaggero, and G. Bertone, Merger rate of a subdominant population of primordial black holes, Phys. Rev. D **98**, 023536 (2018).
[76] B. P. Abbott *et al.* (LIGO Scientific and Virgo Collaborations), Search for subsolar mass ultracompact binaries in Advanced LIGO's second observing run, Phys. Rev. Lett. **123**, 161102 (2019).
[77] V. De Luca, G. Franciolini, P. Pani, and A. Riotto, Primordial black holes confront LIGO/Virgo data: Current situation, J. Cosmol. Astropart. Phys. 06 (2020) 044.
[78] Z.-C. Chen and Q.-G. Huang, Distinguishing primordial black holes from astrophysical black holes by Einstein telescope and cosmic explorer, J. Cosmol. Astropart. Phys. 08 (2020) 039.
[79] O. Pujolas, V. Vaskonen, and H. Veermäe, Prospects for probing gravitational waves from primordial black hole binaries, Phys. Rev. D **104**, 083521 (2021).
[80] I.-K. Chen, M. Kongsore, and K. Van Tilburg, Detecting dark compact objects in Gaia DR4: A data analysis pipeline for transient astrometric lensing searches, J. Cosmol. Astropart. Phys. 07 (2023) 037.
[81] K. Van Tilburg, A.-M. Taki, and N. Weiner, Halometry from astrometry, J. Cosmol. Astropart. Phys. 07 (2018) 041.
[82] H. Verma and V. Rentala, Astrometric microlensing of primordial black holes with gaia, J. Cosmol. Astropart. Phys. 05 (2023) 045.
[83] O. Mena, S. Palomares-Ruiz, P. Villanueva-Domingo, and S. J. Witte, Constraining the primordial black hole abundance with 21-cm cosmology, Phys. Rev. D **100**, 043540 (2019).
[84] P. Villanueva-Domingo and K. Ichiki, 21 cm forest constraints on primordial black holes, Publ. Astron. Soc. Jpn. **75**, S33 (2023).
[85] P. Villanueva-Domingo, O. Mena, and S. Palomares-Ruiz, A brief review on primordial black holes as dark matter, Front. Astron. Space Sci. **8**, 87 (2021).
[86] J. R. Espinosa, T. Konstandin, J. M. No, and G. Servant, Energy budget of cosmological first-order phase transitions, J. Cosmol. Astropart. Phys. 06 (2010) 028.
[87] M. Hindmarsh, S. J. Huber, K. Rummukainen, and D. J. Weir, Gravitational waves from the sound of a first order phase transition, Phys. Rev. Lett. **112**, 041301 (2014).
[88] M. Hindmarsh, S. J. Huber, K. Rummukainen, and D. J. Weir, Numerical simulations of acoustically generated gravitational waves at a first order phase transition, Phys. Rev. D **92**, 123009 (2015).
[89] M. Hindmarsh, S. J. Huber, K. Rummukainen, and D. J. Weir, Shape of the acoustic gravitational wave power spectrum from a first order phase transition, Phys. Rev. D **96**, 103520 (2017); **101**, 089902(E) (2020).
[90] R. Jinno, T. Konstandin, and H. Rubira, A hybrid simulation of gravitational wave production in first-order phase transitions, J. Cosmol. Astropart. Phys. 04 (2021) 014.

[91] R. Jinno, T. Konstandin, H. Rubira, and I. Stomberg, Higgsless simulations of cosmological phase transitions and gravitational waves, J. Cosmol. Astropart. Phys. 02 (2023) 011.

[92] M. Hindmarsh, Sound shell model for acoustic gravitational wave production at a first-order phase transition in the early universe, Phys. Rev. Lett. **120**, 071301 (2018).

[93] M. Hindmarsh and M. Hijazi, Gravitational waves from first order cosmological phase transitions in the Sound Shell Model, J. Cosmol. Astropart. Phys. 12 (2019) 062.

[94] G. Gogoberidze, T. Kahniashvili, and A. Kosowsky, The spectrum of gravitational radiation from primordial turbulence, Phys. Rev. D **76**, 083002 (2007).

[95] C. Caprini, R. Durrer, and G. Servant, The stochastic gravitational wave background from turbulence and magnetic fields generated by a first-order phase transition, J. Cosmol. Astropart. Phys. 12 (2009) 024.

[96] A. Roper Pol, S. Mandal, A. Brandenburg, T. Kahniashvili, and A. Kosowsky, Numerical simulations of gravitational waves from early-universe turbulence, Phys. Rev. D **102**, 083512 (2020).

[97] P. Niksa, M. Schlederer, and G. Sigl, Gravitational waves produced by compressible MHD turbulence from cosmological phase transitions, Classical Quantum Gravity **35**, 144001 (2018).

[98] P. Auclair, C. Caprini, D. Cutting, M. Hindmarsh, K. Rummukainen, D. A. Steer, and D. J. Weir, Generation of gravitational waves from freely decaying turbulence, J. Cosmol. Astropart. Phys. 09 (2022) 029.

[99] C. Caprini *et al.*, Science with the space-based interferometer eLISA. II: Gravitational waves from cosmological phase transitions, J. Cosmol. Astropart. Phys. 04 (2016) 001.

[100] C. Caprini *et al.*, Detecting gravitational waves from cosmological phase transitions with LISA: An update, J. Cosmol. Astropart. Phys. 03 (2020) 024.

[101] D. Bodeker and G. D. Moore, Electroweak bubble wall speed limit, J. Cosmol. Astropart. Phys. 05 (2017) 025.

[102] Y. Gouttenoire, R. Jinno, and F. Sala, Friction pressure on relativistic bubble walls, J. High Energy Phys. 05 (2022) 004.

[103] R. Jinno and M. Takimoto, Gravitational waves from bubble dynamics: Beyond the envelope, J. Cosmol. Astropart. Phys. 01 (2019) 060.

[104] T. Konstandin, Gravitational radiation from a bulk flow model, J. Cosmol. Astropart. Phys. 03 (2018) 047.

[105] M. Lewicki and V. Vaskonen, Gravitational wave spectra from strongly supercooled phase transitions, Eur. Phys. J. C **80**, 1003 (2020).

[106] M. Lewicki and V. Vaskonen, Gravitational waves from colliding vacuum bubbles in gauge theories, Eur. Phys. J. C **81**, 437 (2021); **81**, 1077(E) (2021).

[107] D. Cutting, E. G. Escartin, M. Hindmarsh, and D. J. Weir, Gravitational waves from vacuum first order phase transitions II: From thin to thick walls, Phys. Rev. D **103**, 023531 (2021).

[108] M. Kamionkowski, A. Kosowsky, and M. S. Turner, Gravitational radiation from first order phase transitions, Phys. Rev. D **49**, 2837 (1994).

[109] C. Caprini, R. Durrer, and G. Servant, Gravitational wave generation from bubble collisions in first-order phase transitions: An analytic approach, Phys. Rev. D **77**, 124015 (2008).

[110] S. J. Huber and T. Konstandin, Gravitational wave production by collisions: More bubbles, J. Cosmol. Astropart. Phys. 09 (2008) 022.

[111] R. Jinno and M. Takimoto, Gravitational waves from bubble collisions: An analytic derivation, Phys. Rev. D **95**, 024009 (2017).

[112] D. J. Weir, Revisiting the envelope approximation: Gravitational waves from bubble collisions, Phys. Rev. D **93**, 124037 (2016).

[113] R. Jinno, H. Seong, M. Takimoto, and C. M. Um, Gravitational waves from first-order phase transitions: Ultra-supercooled transitions and the fate of relativistic shocks, J. Cosmol. Astropart. Phys. 10 (2019) 033.

[114] I. Baldes, Y. Gouttenoire, and F. Sala, String fragmentation in supercooled confinement and implications for dark matter, J. High Energy Phys. 04 (2021) 278.

[115] A. Azatov and M. Vanvlasselaer, Bubble wall velocity: Heavy physics effects, J. Cosmol. Astropart. Phys. 01 (2021) 058.

[116] R. Jinno, B. Shakya, and J. van de Vis, Gravitational waves from feebly interacting particles in a first order phase transition, arXiv:2211.06405.

[117] I. Baldes, M. Dichtl, Y. Gouttenoire, and F. Sala, Bubbletrons, Bubbletrons, arXiv:2306.15555.

[118] C. Caprini and D. G. Figueroa, Cosmological backgrounds of gravitational waves, Classical Quantum Gravity **35**, 163001 (2018).

[119] S. R. Taylor, The nanohertz gravitational wave astronomer, arXiv:2105.13270.

[120] J. A. Ellis, M. Vallisneri, S. R. Taylor, and P. T. Baker, Enterprise: Enhanced numerical toolbox enabling a robust pulsar inference suite, Zenodo (2020), https://zenodo.org/record/4059815.

[121] S. R. Taylor, P. T. Baker, J. S. Hazboun, J. Simon, and S. J. Vigeland, enterprise_extensions (2021), v2.3.3.

[122] J. Ellis and R. van Haasteren, jellis18/ptmcmcsampler: Official release, 10.5281/zenodo.1037579 (2017).

[123] R. Z. Ferreira, A. Notari, O. Pujolas, and F. Rompineve, Gravitational waves from domain walls in pulsar timing array datasets, J. Cosmol. Astropart. Phys. 02 (2023) 001.

[124] A. Mitridate, D. Wright, R. von Eckardstein, T. Schröder, J. Nay, K. Olum, K. Schmitz, and T. Trickle, PTArcade, arXiv:2306.16377.

[125] A. Lewis, GetDist: A Python package for analysing Monte Carlo samples, arXiv:1910.13970.

[126] H. Jeffreys, *Theory of Probability* (1939), https://ui.adsabs.harvard.edu/abs/1939thpr.book.....J.

[127] R. E. Kass and A. E. Raftery, Bayes factors, J. Am. Stat. Assoc. **90**, 773 (1995).

[128] G. Agazie *et al.* (NANOGrav Collaboration), The NANOGrav 15 yr data set: Detector characterization and noise budget, Astrophys. J. Lett. **951**, L10 (2023).

[129] H. Kodama, M. Sasaki, and K. Sato, Abundance of primordial holes produced by cosmological first order phase transition, Prog. Theor. Phys. **68**, 1979 (1982).

[130] M. Lewicki, P. Toczek, and V. Vaskonen, Primordial black holes from strong first-order phase transitions, J. High Energy Phys. 09 (2023) 092.

[131] J. Liu, L. Bian, R.-G. Cai, Z.-K. Guo, and S.-J. Wang, Primordial black hole production during first-order phase transitions, Phys. Rev. D **105**, L021303 (2022).

[132] K. Kawana, T. Kim, and P. Lu, PBH formation from overdensities in delayed vacuum transitions, arXiv:2212.14037.

[133] Y. Ali-Haïmoud and M. Kamionkowski, Cosmic microwave background limits on accreting primordial black holes, Phys. Rev. D **95**, 043534 (2017).

[134] V. Poulin, P. D. Serpico, F. Calore, S. Clesse, and K. Kohri, Cmb bounds on disk-accreting massive primordial black holes, Phys. Rev. D **96**, 083524 (2017).

[135] P. D. Serpico, V. Poulin, D. Inman, and K. Kohri, Cosmic microwave background bounds on primordial black holes including dark matter halo accretion, Phys. Rev. Res. **2**, 023204 (2020).

[136] P. Tisserand *et al.* (EROS-2 Collaboration), Limits on the macho content of the galactic halo from the EROS-2 survey of the magellanic clouds, Astron. Astrophys. **469**, 387 (2007).

[137] Y. Gouttenoire, *Beyond the Standard Model Cocktail*, Springer Theses (Springer, Cham, 2022), 10.1007/978-3-031-11862-3.